

Comparable study on typhoon and strong northern wind characteristics of the Runyang Suspension Bridge based on field tests

Wang Hao Li Aiqun Guo Tong Xie Jing Hu Ruomei

(Key Laboratory of Concrete and Prestressed Concrete Structure of Ministry of Education, Southeast University, Nanjing 210096, China)

Abstract: The strong wind characteristics of the Runyang Suspension Bridge (RSB) including the wind speed and direction, the turbulence intensity, the turbulence integral length and power spectrum are analyzed based on measurement data from the wind environment monitoring subsystem of the structural health monitoring system (SHMS) of the RSB and field tests during strong winds. The differences between the typhoon and the strong northern wind are especially studied. It is found that the mean wind speed of the strong northern wind is a little smaller and the mean wind direction is more stable than that of the typhoon. The turbulence intensity of both the typhoon and the strong northern wind is greater than the values suggested in Chinese code, and the turbulence integral length difference between the typhoon and a strong northern wind is not clear. As for the along-wind turbulence power spectrum, the spectrum of the strong northern wind can fit the Kaimal spectrum better than that of the typhoon. The obtained results can provide measurement data for founding a strong wind characteristic database and determining the strong wind characteristic parameter values of the RSB.

Key words: suspension bridge; typhoon; northern wind; wind characteristics; field test; structural health monitoring system

In order to accurately calculate the wind effect on structures, the wind characteristics on the structures must be accurately simulated first. These characteristics mainly include the mean wind characteristics and the turbulence wind characteristics. The mean wind characteristics contain the mean wind speed and direction, the wind speed variation with altitude, etc. The turbulence wind characteristics contain the turbulence intensity, the turbulence integral length, the power spectrum density function, etc. However, the most effective measure of obtaining the regional wind characteristics is to conduct considerable wind measurements, and then to analyze the measurement data using statistical methods. Therefore, experimental studies on strong wind characteristics are of great value to the development of wind engineering^[1-3].

Much progress on wind climate studies has been achieved in some foreign countries since the 1970s and parts of the wind characteristics database have been established, but most of the database is for meteorological applications^[4-5]. In

China, only a few measurement studies have been conducted^[6-10], so many wind characteristic parameters are determined by foreign research results. It is obviously unreasonable because the wind characteristics are sensitive to site location. Therefore, it is especially significant and necessary to carry out field tests on strong wind characteristics in sites in China.

Meteorological study shows that the strong wind load affecting the Runyang Suspension Bridge (RSB) mainly concerns typhoons happening in the summer and northern winds in the winter. During the last three years, the RSB has suffered from typhoons and strong northern winds many times. In order to master the strong wind characteristics, the data from both the SHMS and field tests are applied to conduct comparable studies on typhoon and strong northern wind characteristics at the spot of the RSB. The research results are also compared with the existing wind resistance criteria of the bridges^[11], which can provide not only measurements for wind resistance safety assessments of the RSB, but also references for wind resistance designs of other long span bridges, especially bridges crossing the Yangtze River in Jiangsu province.

1 Background

As a national key engineering project, the Runyang Yangtze River Bridge which connects Zhenjiang city with Yangzhou city is composed of two long span bridges. One is the RSB located in the south and the other is the Runyang Cabled-Stayed Bridge (RCB) in the north of the Yangtze River. The RSB is a single-span hinged and simply supported steel-box-girder bridge with a main span of 1 490 m as shown in Fig. 1. It is the longest suspension bridge in China and the third longest in the world^[10].

Meteorological studies carried out by Meteorology Research Institute of Jiangsu Province in June 2000 show that the RSB is located in the northern region of the subtropical zone, which has obvious subtropical monsoon climate characteristics. The cold and dry northern wind from the mainland is the main strong wind in winter, and in summer the strong wind is dominated by the typhoon from the sea; spring and autumn are the monsoon conversion seasons. The climate of the RSB spot is complex and there are many disastrous weather conditions including drought, flooding, cold waves, hail, typhoons, storms, cryogenic freeze injury, thunderstorms, squall lines, etc^[12].

In order to monitor and assess the health conditions of the RSB during the building and operating period, especially the conditions under the influence of disasters, the Structural Health Monitoring Institute of Southeast University has taken charge of designing the SHMS of the Runyang Suspension Bridge. Fig. 1 shows the sensor layout in the

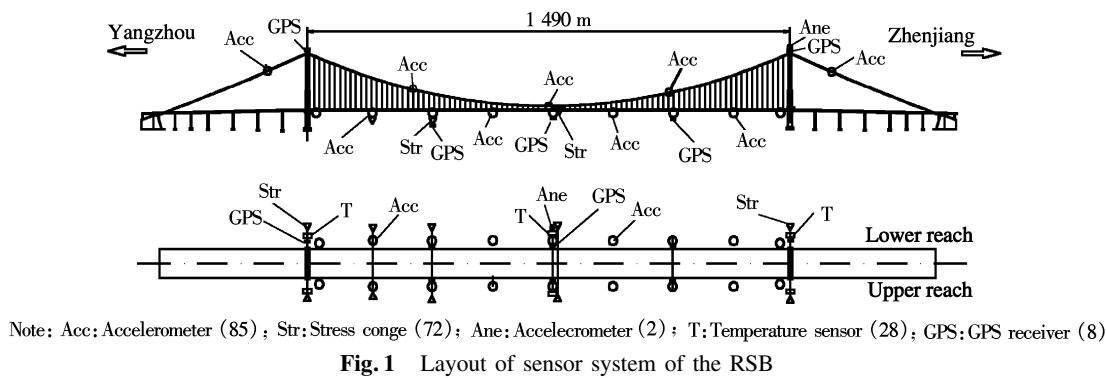
Received 2008-08-13.

Biography: Wang Hao (1980—), male, doctor, lecturer, whzjn@sina.com.

Foundation items: The National High Technology Research and Development Program of China (863 Program) (No. 2006AA04Z416), the Key Project of the National Natural Science Foundation of China (No. 50538020), the National Science Fund for Distinguished Young Scholars (No. 50725828), the National Natural Science Foundation of China for Young Scholars (No. 50608017), the Ph.D. Programs Foundation of Ministry of Education of China (No. 200802861012).

Citation: Wang Hao, Li Aiqun, Guo Tong, et al. Comparable study on typhoon and strong northern wind characteristics of Runyang Suspension Bridge based on field tests[J]. Journal of Southeast University (English Edition), 2009, 25(1): 99 – 103.

SHMS. In order to achieve measurement wind data and to provide reliable bases for wind resistance evaluations for the RSB, two anemometers are installed, as shown in Fig. 1. The numbers in brackets mean the quantity of sensors.



2 Anemometers and Measurement Locations

Two kinds of anemometers are applied in the field wind test, the WA15 anemometer from the Vaisala Company and the 1590-PK-020 3-D sonic anemometer from Gill Instruments Limited.

Two WA15 anemometers are adopted in the SHMS of the RSB, as shown in Fig. 2. One is employed on the top of the south tower(downstream) about 218. 905 m above the ground and the other is in the middle of the main span(up-stream) about 69. 300 m above the ground. The anemometers are installed facing the north, with the angle of wind direction defined by 0° corresponding to the north. According to clockwise rotation, the east is 90° and so forth. Long-term successful applications in meteorological studies show that the WA15 anemoscope can function under all kinds of bad weather and can accurately measure the wind speed and direction.

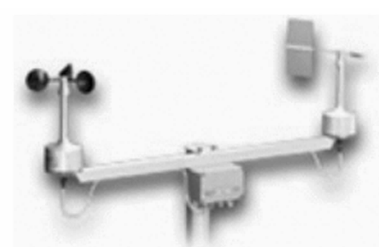


Fig. 2 WA15 anemometer

Three 1590-PK-020 3-D sonic anemometers (shown in Fig. 3) are adopted in the field test by the research members during the strong winds. The 1590-PK-020 anemometer with light weight and small volume is especially fit for working in the rain. The maximum sampling frequency is 100 Hz. All of above specifications make the 1590-PK-020 anemometer be comprehensively used in wind tests of engineering structures. Because these three anemometers can be installed on any location of the RSB according to the measurement object, the turbulence integral length and spatial correlation of a strong wind can be measured.

3 Comparable Study on Measurement Typhoon and Strong Northern Wind Characteristics

During the last three years, the SHMS of the RSB has recorded four typhoons and more than 10 occurrences of

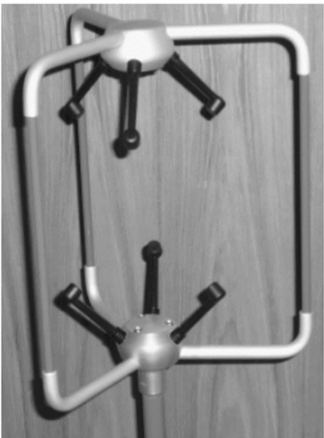


Fig. 3 1590-PK-020 anemometer

strong northern winds. Two kinds of strong winds are compared and analyzed. The typhoon Matsa in August, 2005 and Wipha in September, 2007 are selected as two typical typhoon examples at the RSB spot. Because of the similarities of the strong northern wind characteristics, only the measurement data recorded in March, 2007 are applied.

3. 1 Mean wind speed and direction

In the wind engineering studies, the turbulence wind speed is assumed as an ergodic process, so the whole sample mean can be replaced by a single sample time mean. During the analysis, 10-min is taken as a basic interval, and the period when the wind speed is the strongest and comparatively stable is selected. The analysis results of the mean wind speed and the direction of the three strong winds are shown in Tab. 1 and Tab. 2, respectively.

Tab.1 Maximum of the 10-min mean wind speed m/s		
Typhoon Matsa	Typhoon Wipha	Northern wind
17. 86	13. 43	10. 91

Tab.2 Variation of the 10-min mean wind direction (°)		
Typhoon Matsa	Typhoon Wipha	Northern wind
< 50	< 40	< 25

As shown in Tab. 1, both of the wind speeds of the two typhoons are greater than that of the strong northern wind. Because the center of typhoon Matsa went through the RSB, the wind speed is obviously larger than that of ty-

phoon Wipha. And Tab. 2 shows that the strong northern wind direction is more stable than that of the two typhoons.

3.2 Turbulence intensity

The turbulence flow is an extremely irregular movement, so in the structural wind engineering research, it is often divided into the mean wind and the turbulence wind in order to simplify the analysis. As one of the key parameters reflecting the turbulence characteristic, the turbulence intensity I is used to represent the ratio of the turbulence value by the mean value.

$$I_i = \frac{\sigma_i}{U} \quad i = u, v, w \tag{1}$$

where U means the mean wind speed; u, v and w represent along-wind, across-wind and vertical, respectively; σ_u, σ_v and σ_w represent the average variety of ranges of the turbulence wind (mean square deviation) in three directions (along-wind, across-wind and vertical direction); I_u, I_v and I_w represent the turbulence intensities in the above three directions. Therefore, according to Eq. (1), it is easy to calculate the turbulence intensity values using the measurement wind data.

In order to carry out a comparable study, the maximum and the average of the 10-min turbulence intensity of the three strong winds are shown in Tab. 3 and Tab. 4, respectively.

Tab.3 Maximum of the 10-min turbulence intensity %

Strong wind	I_u	I_v	I_w
Typhoon Matsa	23.02	20.22	
Typhoon Wipha	29.37	26.69	13.13
Northern wind	31.03	24.66	

Tab.4 Average of the 10-min turbulence intensity %

Strong wind	I_u	I_v	I_w
Typhoon Matsa	10.95	10.44	
Typhoon Wipha	19.72	18.66	8.76
Northern wind	14.98	13.67	

The wind resistance criteria of the bridges suggest that the along-wind turbulence intensity at 50 to 70 m above the ground in the open water field is about 11%. As can be seen in Tab. 3 and Tab. 4, the turbulence intensities of both the typhoon Wipha and the strong northern wind are greater than 11%. In addition, the criteria suggest that I_v is equal to $0.88I_u$ when there is no measurement data, but all of the strong wind measurement data show that I_v is greater than $0.9I_u$, so the existing criteria are not completely fit for the RSB in the turbulence intensity aspect.

3.3 Turbulence integral length

The turbulence integral length usually fluctuates in a large range. Based on the measurement strong wind data, the along-wind turbulence integral length L_u^x and the across-wind turbulence integral length L_v^x are all calculated using the auto-correlation function integral method^[1]. The integral is finished when the correlation coefficient declines to less

than 0.05. The maximum, average, minimum and the range of the 10-min turbulence integral length of the three strong winds are shown in Tabs. 5 to 8, respectively.

Tab.5 Maximum of the 10-min turbulence integral length m

Strong wind	L_u^x	L_v^x
Typhoon Matsa	197.8	78.6
Typhoon Wipha	282.5	173.1
Northern wind	217.3	169.9

Tab.6 Average of the 10-min turbulence integral length m

Strong wind	L_u^x	L_v^x
Typhoon Matsa	68.4	35.6
Typhoon Wipha	119.7	77.6
Northern wind	99.6	48.1

Tab.7 Minimum of the 10-min turbulence integral length m

Strong wind	L_u^x	L_v^x
Typhoon Matsa	13.2	8.9
Typhoon Wipha	17.4	10.5
Northern wind	24.7	9.7

Tab.8 Range of the 10-min turbulence integral length m

Strong wind	L_u^x	L_v^x
Typhoon Matsa	20 to 160	10 to 80
Typhoon Wipha	60 to 180	30 to 130
Northern wind	50 to 170	20 to 100

As can be seen in Tabs. 5 to 8, the turbulence integral length of the strong northern wind is often larger than that of typhoon Matsa and less than that of typhoon Wipha, so there are no clear regularities between the typhoon and the strong northern wind with respect to the turbulence integral length. This conclusion needs to be further proved by future measurement studies.

In order to illustrate the turbulence integral length of the typhoon more clearly, Fig. 4 and Fig. 5 show the turbulence integral length distribution probability of typhoon Matsa and typhoon Wipha, respectively. In Fig. 4 and Fig. 5, the x -axis represents the turbulence integral length and the y -axis represents the corresponding distribution probability.

3.4 Turbulence power spectrum density

The power spectral density function can accurately reflect the corresponding contribution of various frequencies of the turbulence and is the basis of turbulence wind field simulation, so it is one of the most important turbulence wind characteristics. One important method to acquire the turbulence power spectral density function is to carry out the function fitting based on the statistical analysis of the massive measurement wind records.

Davenport simulated the along-wind turbulence wind spectrum based on more than 90 times of strong wind data recorded in different places of the world and at different altitudes, and then the spectrum was modified and perfected by many scholars. The current wind resistance criteria of the bridges adopts the Kaimal spectrum which was presented by Kaimal in 1972. If the wind speed at the Z altitude is U , then the along-wind turbulence wind power spectrum density function can be expressed as

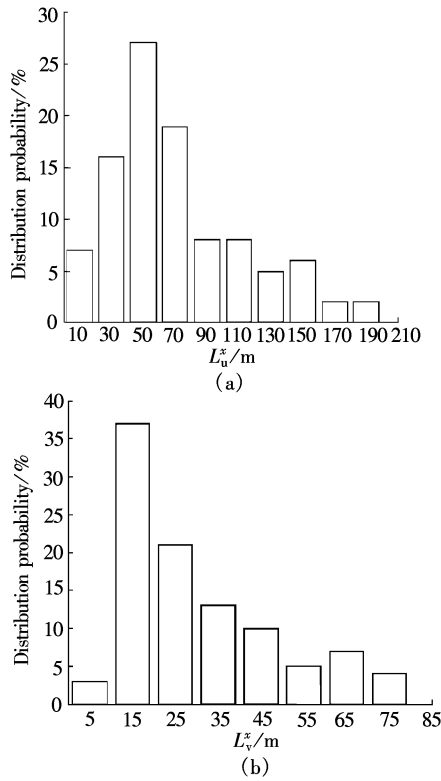


Fig. 4 10-min turbulence integral length of typhoon Matsa. (a) L_u^x ; (b) L_v^x

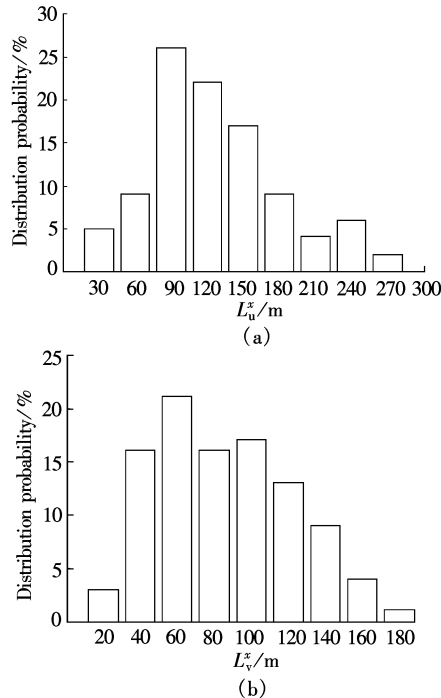


Fig. 5 10-min turbulence integral length of typhoon Wipha. (a) L_u^x ; (b) L_v^x

$$\frac{nS_u(n)}{(u^*)^2} = \frac{200f}{(1 + 50f)^{5/3}} \quad (2)$$

$$f = nZ/U \quad (3)$$

where S_u is the auto-power spectral density of along-wind turbulence; n is the frequency of the wind speed; Z is the height of the wind speed relative to the sea level; u^* is the wind friction speed; f is the Mourning coordinate. Because

there is no measurement data of u^* in the field wind test of the RSB, the value of u^* can be calculated according to the energy unitary method as follows^[2]:

$$\sigma_u^2 = 6(u^*)^2 \quad (4)$$

During the turbulence wind power spectrum analysis, the size of the fast Fourier transform (FFT) is 1 024 with a frequency increment of 1.75 mHz between two adjacent data points. The piecewise smoothing method and the Hamming window are adopted and the nonlinear least-squares fitting technique is used to reduce the random error of spectral estimates. Figs. 6 to 8 show the comparisons of turbulence power spectrum functions between the measurements, three strong winds and the Kaimal spectrum, respectively.

Figs. 6 to 8 show that all of the three kinds of turbulence power spectrum density functions of the measurement of the strong wind cannot coincide with the Kaimal spectrum well. As for typhoon Matsa, it is a little smaller in the low

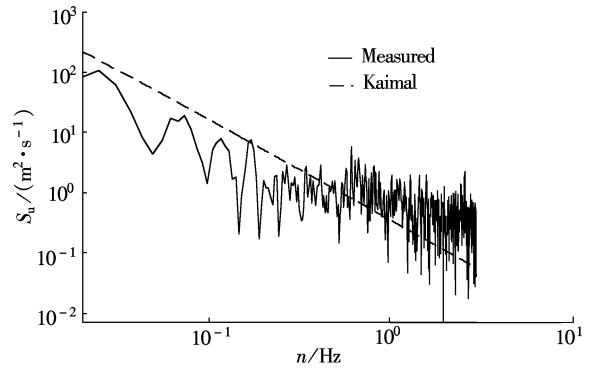


Fig. 6 Comparison of the turbulence power spectra of typhoon Matsa and Kaimal spectra

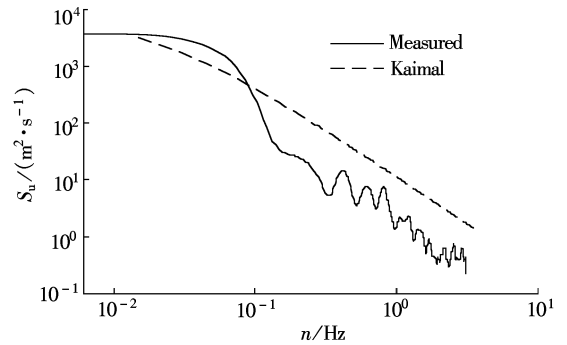


Fig. 7 Comparison of the turbulence power spectra of typhoon Wipha and Kaimal spectra

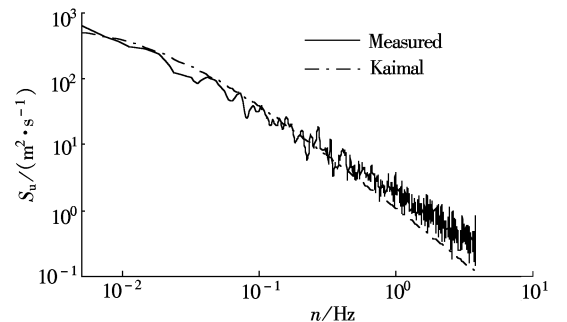


Fig. 8 Comparison of the turbulence power spectra of the strong northern wind and Kaimal spectra

frequency domain and a little larger in the high frequency domain, which shows that the horizontal turbulence kinetic energy distribution of typhoon Matsa offsets to the high domain. The turbulence power spectrum density of typhoon Wipha is just converse to that of typhoon Matsa. Relatively, the along-wind turbulence power spectrum of the strong northern wind can fit the Kaimal spectrum better than that of the typhoon.

4 Conclusions

1) The wind speeds of the two typhoons are larger than that of the strong northern wind, so the typhoon in summer is the dominant wind load on the RSB. And the strong northern wind direction is more stable than those of the two typhoons.

2) The measured along-wind turbulence intensity of both typhoon Wipha and the strong northern wind are larger than values suggested by the current wind resistance criteria of the bridges. In addition, all of the strong wind measurement data show that I_v is greater than $0.9I_u$, so the current criterion is not completely suitable for the RSB with regard to turbulence intensity.

3) The integral length of the strong northern wind is usually larger than that of typhoon Matsa and less than that of typhoon Wipha, so the relationship between typhoon and strong winds is not clear. This conclusion needs to be further proved by future measurement studies.

4) All of the three kinds of turbulence power spectrum density functions of the measured strong wind cannot coincide with Kaimal spectra well, but the along-wind turbulence power spectrum of the strong northern wind can fit the Kaimal spectrum better than that of the other typhoons.

References

[1] Xiang Haifan. *Modern theory and practice on bridge wind resistance* [M]. Beijing: China Communications Press,

2005. (in Chinese)

- [2] Simiu E, Scanlan R H. *Wind effects on structures* [M]. New York: John Wiley & Sons, 1996.
- [3] Chen Zhengqing. *Wind engineering of bridges* [M]. Beijing: China Communications Press, 2005. (in Chinese)
- [4] Harikrishna P, Annadurai A, Gomathinayagam. Full scale measurements of the structural response of a 50 m guyed mast under wind loading [J]. *Engineering Structures*, 2003, **25**(7): 859 – 867.
- [5] Pang Jiabin, Lin Zhixing, Ge Yaojun. Field measurements of strong wind characteristics in Pudong district [J]. *Experiments and Measurements in Fluid Mechanics*, 2002, **16**(3): 32 – 39. (in Chinese)
- [6] Xu Y L, Zhu L D, Wong K Y. Field measurement results of Tsing Ma Suspension Bridge during typhoon Victor [J]. *Structural Engineering and Mechanics*, 2000, **10**(6): 545 – 559.
- [7] Law S S, Bu J Q, Zhu X Q. Wind characteristics of typhoon Dujuan as measured at a 50 m guyed mast [J]. *Wind and Structures*, 2006, **9**(5): 387 – 396.
- [8] Li Q S, Wu J R, Liang S G, et al. Full-scale measurements and numerical evaluation of wind-induced vibration of a 63-story reinforced concrete super tall building [J]. *Engineering Structures*, 2004, **26**(12): 1779 – 1794.
- [9] Wang Yayong, Zhang Ziping, He Jun, et al. Measurements on wind and dynamic properties of Diwang Plaza in Shenzhen city [J]. *Journal of Building Structures*, 1998, **19**(3): 58 – 63. (in Chinese)
- [10] Li Aiqun, Wang Hao, Xie Yishun. Experimental study on strong wind characteristics of Runyang Suspension Bridge based on SHMS [J]. *Journal of Southeast University: Natural Science Edition*, 2007, **37**(3): 508 – 511. (in Chinese)
- [11] Xiang Haifan. *Bridge wind resistance guide for the highway bridges* [M]. Beijing: China Communications Press, 1996. (in Chinese)
- [12] Meteorology Research Institute of Jiangsu Province. Preliminary design study report on Runyang Yangtze River Bridge (special topic for wind speed observation) [R]. Nanjing: Meteorology Research Institute of Jiangsu Province, 2002. (in Chinese)

基于现场实测的润扬悬索桥桥址区台风与强北风特性对比

王 浩 李爱群 郭 彤 谢 静 胡若玫

(东南大学混凝土及预应力混凝土结构教育部重点实验室, 南京 210096)

摘要:综合利用润扬结构健康监测系统(SHMS)风环境子系统实时记录的各种参数时程数据以及强风期间上桥实测强风样本,分析得到了桥址区实测强风的风速和风向、紊流强度、紊流积分尺度、紊流功率谱密度函数等特性,重点对比研究了台风与强北风特性之间的差异性.结果表明,与台风相比,强北风的平均风速略小、平均风向更加稳定;台风与强北风的实测紊流强度值均比规范建议值大;台风与强北风的紊流积分尺度之间无明显的规律性;就顺风向紊流功率谱而言,强北风与 Kaimal 谱更加吻合.研究结果为建立桥址区台风特性数据库,确定当地强风特性参数的合理取值提供了实测依据.

关键词:悬索桥;台风;北风;风特性;现场实测;结构健康监测系统

中图分类号:U448;V321